# Magnetotransport in doped manganate perovskites

by J. Z. Sun
L. Krusin-Elbaum
A. Gupta
Gang Xiao
P. R. Duncombe
S. S. P. Parkin

Recent progress in oxide perovskite thin-film technology has led to the discovery of a large negative magnetoresistance at room temperature in doped manganate perovskite thin films. These films may have potentials for magnetic sensing applications. In this paper we review the basic phenomena and physics of magnetotransport in this class of materials. We also discuss our recent demonstration of a large low-field magnetoresistance effect, and the associated challenges that lie ahead.

#### Introduction

Large magnetoresistance (MR) was observed in the 1970s and 1980s in bulk ceramic and single-crystal forms of doped manganate perovskites. Kusters et al. [1] observed a negative magnetoresistance in the bulk doped perovskite manganate  $Nd_{0.5}Pb_{0.5}MnO_3$ , for which a magnetic-field-induced percentage change in resistance  $\Delta R/R(H=0) > 50\%$  was found near its ferromagnetic transition at a temperature of 184 K. Here R(H=0) is the resistance in zero field H=0, and  $\Delta R=R(H=0)-R(H\neq0)$ . A negative magnetoresistance is defined as  $R(H=0) > R(H\neq0)$ . Earlier, Searle and Wang [2] had reported spin-dependent metal-insulator transitions in single crystals of (LaPb)MnO<sub>3</sub>.

The recent interest in magnetoresistance in doped perovskite manganates was initiated by the discovery of a large room-temperature magnetoresistance in epitaxial thin films [3]. Thin films with large magnetoresistance at

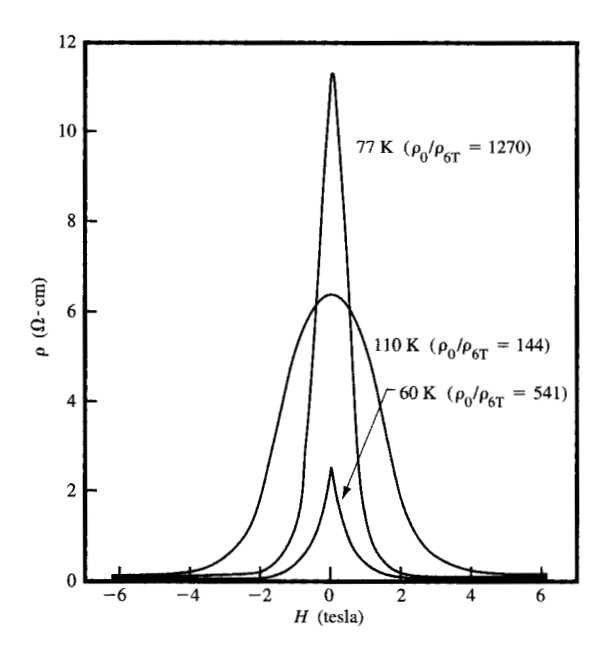
room temperature open up new possibilities for applications in diverse areas of technology such as magnetic random access memories and read heads for hard disk drives. Thin-film deposition technology for complex oxide materials has seen rapid progress, thanks to the effort in the commercialization of the high-temperature superconductors—a class of doped cuprate perovskites with materials characteristics similar to those of the doped manganate perovskites.

Successful synthesis of the doped manganate perovskite thin films dates back to at least 1990, when Kasai and Ohno [4] first reported their work on the superconducting proximity effect observed in sandwiched epitaxial YBa<sub>2</sub>Cu<sub>3</sub>O<sub>7</sub>/La<sub>0.7</sub>Ca<sub>0.3</sub>MnO<sub>3</sub>/YBa<sub>2</sub>Cu<sub>3</sub>O<sub>7</sub> thin films. Also in 1990, Cho et al. [5] reported successful deposition of La<sub>0.7</sub>Sr<sub>0.3</sub>MnO<sub>3</sub> in epitaxial form using rf diode magnetron sputtering.

In 1993, Von Helmolt et al. [3] reported a large negative magnetoresistance effect, of the order  $\Delta R/R(H=0) > 60\%$  at room temperature in a 7-tesla field, in laser-deposited thin-film  $\mathrm{La_{0.67}Ba_{0.33}MnO_x}$ . This was soon followed by the report of McCormack et al. [6] and Jin et al. [7] of their findings that thin-film  $\mathrm{La_{0.67}Ca_{0.33}MnO_3}$  exhibits  $\Delta R/R(H=6~\mathrm{T})=127000\%$  at 77 K. This large magnetoresistance effect has since been referred to as "colossal magnetoresistance" (CMR). In these early studies, a postdeposition anneal was critical for obtaining large magnetoresistance [3, 6, 7]. A typical annealing condition involves a high-temperature (around 900°C) short-time (about 30 min) treatment in an oxygen atmosphere.

Copyright 1998 by International Business Machines Corporation. Copying in printed form for private use is permitted without payment of royalty provided that (1) each reproduction is done without alteration and (2) the Journal reference and IBM copyright notice are included on the first page. The title and abstract, but no other portions, of this paper may be copied or distributed royalty free without further permission by computer-based and other information-service systems. Permission to republish any other portion of this paper must be obtained from the Editor.

0018-8646/98/\$5.00 © 1998 IBM



#### Flaure

Example of the large magnetoresistance observed in an annealed  $La_{0.67}Ca_{0.33}MnO_3$  epitaxial thin film. Data from McCormack et al. [6]. Reproduced from [6], with permission.

Soon afterward it was demonstrated that chemical substitution on the trivalent site could have an effect equivalent to a controlled anneal. With 7% replacement of lanthanum by yttrium, Jin et al. [8] showed that large magnetoresistance with  $\Delta R/R(H=6~\rm T)\sim 10^3$  can also be obtained in samples of bulk ceramic form at a temperature close to 140 K. Sun et al. [9] demonstrated that, using the same 7% yttrium substitution, values of  $\Delta R/R(H=6~\rm T)$  as high as ~200 can be obtained around 100 K with as-grown thin films that were laser-deposited at  $600^{\circ}\rm C$  without postdeposition anneal.

For CMR effects in both bulk and thin-film materials, the basic phenomena seem to be the same. The resistivity peaks near the Curie temperature, around which the largest magnetoresistance is obtained. Above the Curie temperature, the resistivity shows a thermally activated behavior [10]. Below the Curie temperature, the resistivity decreases with decreasing temperature as the magnetic moment grows. A correlation has been found between the resistivity and magnetization [9, 11, 12]. A larger pseudoperovskite cell size seems to correlate with a lower Curie temperature, and a lower Curie temperature leads to a higher resistivity peak, which is accompanied by a larger magnetoresistance effect. All reports of large magnetoresistances involve the preparation of the

materials in such a way as to suppress its resistance-peak temperature to below 150 K.

The saturation magnetic field necessary to achieve a full CMR effect in the generic materials is large, usually of the order of several tesla, as illustrated in **Figure 1**. This limitation has recently been overcome for temperatures below 100 K, when large magnetoresistances in low fields were demonstrated in trilayer manganate/SrTiO<sub>3</sub>/manganate devices [13].

In this paper, we review the current state of affairs in this very dynamic area of research. We summarize some basic materials data established to date, as well as some of the building blocks of our understanding. We discuss in greater detail the issues we have highlighted above, especially with regard to the possible mechanism that produces the CMR effect and its implications for low-field magnetoresistance in the manganates.

#### Materials properties

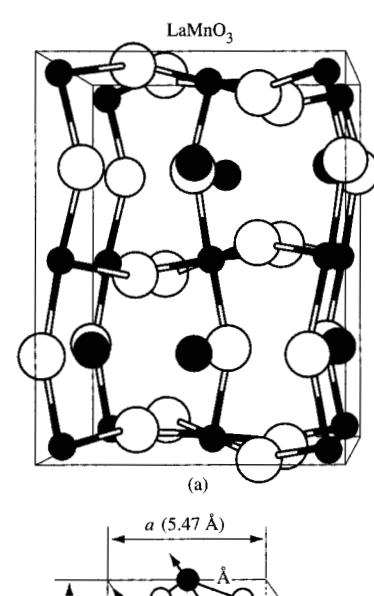
Manganate perovskite oxides were first systematically studied in the 1950s [14, 15]. The parent compounds  ${\rm La^{3+}Mn^{3+}O_3}$  and  ${\rm Ca^{2+}Mn^{4+}O_3}$  both have a perovskite structure.  ${\rm La^{3+}Mn^{3+}O_3}$  is a layered antiferromagnet, while  ${\rm Ca^{2+}Mn^{4+}O_3}$  is an antiferromagnet with opposite spin orientations for nearest-neighbor  ${\rm Mn^{4+}}$  spins [18].

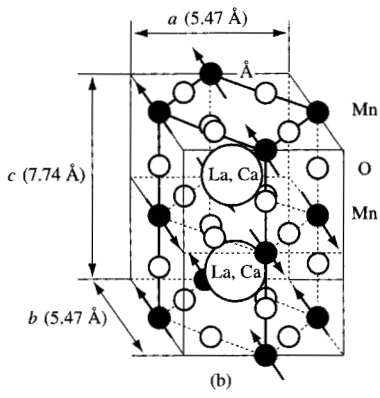
La<sup>3+</sup>Mn<sup>3+</sup>O<sub>3</sub> is an antiferromagnetic insulator; Figure 2(a) is a schematic of its cell structure. A Jahn-Teller distortion lifts the double degeneracy of the  $E_g$  orbitals and defines the direction along which the Mn3+ moments order antiferromagnetically. A schematic of the layered antiferromagnetic Mn<sup>3+</sup> moment arrangement is shown in Figure 2(b). From neutron diffraction studies, Wollan et al. [18] concluded that the Mn<sup>3+</sup> moment must in this case lie in the plane of the Mn-O sheet, although the relative orientation of the moment with respect to the cell edge could not be determined from powder diffraction data. Recent work on thin-film La<sub>0.7</sub>Sr<sub>0.3</sub>MnO<sub>3</sub> grown using laser ablation [19] suggests that a magnetic easy axis may exist for the magnetic moments to align along the (110) direction of the pseudocubic perovskite cell, as shown in Figure 2(b). CaMnO, is also an antiferromagnetic insulator, with a Mn4+ moment aligned antiferromagnetically with a cubic symmetry [18]. It has a Neel temperature of 120 K.

Between these two end compounds exists a continuous solid solution whose structural, magnetic, and transport properties depend sensitively on doping level x.

Figure 3(a) shows a summary of the lattice constant of  $\text{La}_{1-x}\text{Ca}_x\text{MnO}_3$  as a function of x. The Jahn-Teller distortion-related orthorhombicity disappears for x above 0.2, around which a metallic conductivity sets in, together with a large increase of the ferromagnetic moment.

The magnetic phase diagram of the  $La_{1-x}Ca_xMnO_3$  system is shown in **Figure 3(b)** [20]. This phase diagram

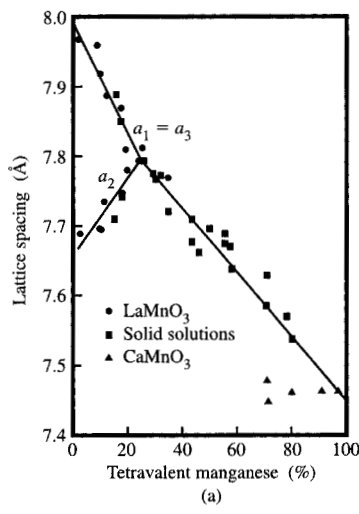


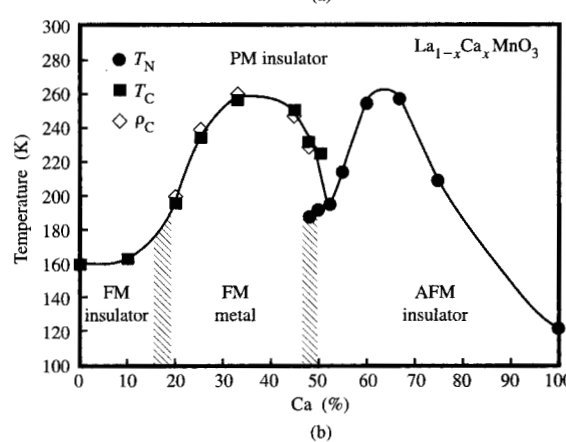


#### Floure 2

(a) Sketch of the Jahn-Teller distorted LaMnO<sub>3</sub> lattice structure, redrawn according to Pickett and Singh [16]; (b) alignment of magnetic moment of Mn<sup>3+</sup> ions, according to the drawing of Chahara et al. [17] based on Wollan's neutron study [18]. Part (a) reproduced from [16], with permission; part (b) reproduced from [17], with permission.

is also qualitatively true for other manganate perovskites such as  $\text{La}_{1-x}\text{Ba}_x\text{MnO}_3$  and  $\text{La}_{1-x}\text{Sr}_x\text{MnO}_3$  [21–23]. The Curie temperature peaks around  $x \sim 0.3$ . The maximum Curie temperature of 380 K was observed in  $\text{La}_{0.7}\text{Sr}_{0.3}\text{MnO}_3$  [22, 24]. **Table 1** contains a summary of some representative compounds with  $x \approx 0.3$  [24]. Around  $x \sim 0.5$ , the system exhibits a complex first-order ferromagnetic–antiferromagnetic transition, accompanied by a metal–insulator transition [25–29]. Long-range ordering of the dopant charge is believed to exist at this doping level and is responsible for the first-order phase transition.  $\text{Pr}_{1-x}\text{Ba}_x\text{MnO}_3$ ,  $\text{Nd}_{1-x}\text{Sr}_x\text{MnO}_3$ , and  $\text{La}_{1-x}\text{Pb}_x\text{MnO}_3$  have also been studied at selected compositions [10], particularly around  $x \sim 0.3$  and  $x \sim 0.5$ .





#### E la tiva d

(a) Lattice parameter of  $La_{1-x}Ca_xMnO_3$  as a function of x (represented in % of  $Mn^{4+}$ , redrawn from Wollan et al. [18]; (b) Magnetic phase diagram of  $La_{1-x}Ca_xMnO_3$ . From Schiffer et al. [20]. Part (a) reproduced from [18], with permission; part (b) reproduced from [20], with permission.

The  $\text{La}_x \text{MnO}_{3-\delta}$  (0.67  $\leq x \leq 1$ ) self-doped system also exhibits ferromagnetic ordering, with a maximum Curie temperature around 300 K [30, 31].

The magnetic and transport properties of doped manganate perovskites show a sensitive pressure dependence. Upon the application of hydrostatic pressure, the Curie temperature rises, the resistivity decreases, and the effective amount of magnetoresistance decreases. Results for polycrystalline  $Pr_{0,7}Ca_{0,3}MnO_3$  and for  $La_{0,7}Ca_{0,3}MnO_3$  were reported by Hwang et al. [32]. Pressure-dependence studies of other systems have also been reported. Arnold et al. [33] reported hydrostatic-pressure-dependent magnetic and transport properties of

**Table 1** Physical properties of  $(A_{0.7}^{3+}B_{0.3}^{2+})$ MnO<sub>3</sub> compounds, according to Coey et al. [24].

System	a <sub>0</sub> a (nm)	Т <sub>с</sub> (К)	$\gamma^b$ (mJ-mol <sup>-1</sup> K <sup>2</sup> )	$\theta_D^{\mathfrak{h}}$ (K)	$ ho_0 \ (\Omega ext{-m})$
$(Y_{0.7}Sr_{0.3})MnO_3$	0.3858(4)	360(5)	8.1(3)	348(5)	$5 \times 10^{-8}$
$(La_{0.7}Sr_{0.3})MnO_3$	0.3875	370	6.0	353	$6 \times 10^{-7}$
$(La_{0.7}Ba_{0.3})MnO_3$	0.3885	330	6.1	333	$1 \times 10^{-6}$
$(La_{0.7}Ca_{0.3})MnO_3$	0.3855	220			$1 \times 10^{-4}$
$(La_{0.7}Ca_{0.3})MnO_3^b$	0.3860	260	5.2		$2 \times 10^{-4}$
$(Nd_{0.7}Ba_{0.3})MnO_3^b$	0.3883	145			$7 \times 10^{-1}$
$(Nd_{0.7}Sr_{0.3})MnO_3$	0.3872	115			$8 \times 10^{1}$
$(Nd_{0.7}Ba_{0.3})MnO_3$	0.3885	110			$8 \times 10^3$

aLattice parameter of the elementary perovskite cell.

polycrystalline La $_{0.60}$ Y $_{0.07}$ Ca $_{0.33}$ MnO $_3$ , and obtained an average  $dT_c/dP$  of around 2.5 K/kbar for  $T_c$  around 160 K. Khazeni et al. [34] studied the hydrostatic pressure dependence of magnetotransport in single-crystal Nd $_{0.5}$ Sr $_{0.36}$ Pb $_{0.14}$ MnO $_{3-\delta}$ , and found a  $dT_c/dP$  of 1.9 K/kbar for a  $T_c$  around 200 K. All three studies reveal a positive  $dT_c/dP$ , around 2 K/kbar.

The structural properties of the doped manganate perovskites show a strong correlation to their magnetic state. When the value of doping level x is increased, a metallic and ferromagnetic state develops, accompanied by a diminishing orthorhombic distortion. This can be seen in Figure 3(a), where the difference in  $a_1$  and  $a_2$  virtually disappears for  $x \ge 0.2$ . Significant changes in lattice constants also occur when samples go through their ferromagnetic transition. Radaelli et al. [35] observed a large magnetovolume effect in polycrystalline samples of  $La_{1-x}Ca_xMnO_3$  with x = 0.25 and 0.50. For x = 0.25, a lattice contraction immediately below the Curie temperature was observed, with a volume discontinuity of  $\Delta V/V \approx 0.13\%$ . For samples with x = 0.50, a much larger discontinuity was observed in lattice constants at the antiferromagnetic-to-ferromagnetic transition of 160 K, but with very little net volume change. For single-crystal  $La_{1-x}Sr_xMnO_3$  at x = 0.170, Asamitsu et al. [36] reported a first-order structural phase transition between the orthorhombic form (low temperature, ferromagnetic) and the rhombohedral form (high temperature, paramagnetic) that can be triggered either by varying temperature near the Curie point or by the application of a magnetic field of the order of 1 tesla. A more dramatic first-order striction-coupled metal-insulator phase transition was observed in the single-crystal compound of  $(Nd_{1...y}Sm_y)_{1/2}Sr_{1/2}MnO_3$  at y = 0.938, for which a resistivity change of more than three orders of magnitude, from 20  $\Omega$ -cm to 4  $\times$  10<sup>-4</sup>  $\Omega$ -cm, was observed at the Curie temperature of 110 K [25]. Near the Curie temperature, the phase transition could be driven by the

application of a relatively small magnetic field. In a low field of 2.5 kOe, a  $\Delta R/R(H)$  of 100 was observed within a narrow temperature range of a few degrees above the Curie temperature.

New compounds with similar magnetic and transport behaviors are rapidly being discovered. Moritomo et al. [37] recently reported successful synthesis of the layered perovskite system  $(La_{1-x}Sr_x)_{n+1}Mn_nO_{3n+1}$ . A resistance change of close to two orders of magnitude in 7 tesla of field was demonstrated for the n = 2 compound at x = 0.4 near its Curie temperature of around 130 K. Additionally, a large magnetoresistance was observed in the pyrochlore compound Tl<sub>2</sub>MnO<sub>7-8</sub>, which has a Curie temperature around 150 K [38, 39]. Hall measurements [38] indicate that the majority carriers are electrons in  $Tl_2MnO_{7-8}$ , and the carrier density is only 0.001–0.005 conduction electrons per formula unit. This is in contrast to the doped perovskite manganates, for which the conduction carriers are holes and the doping density is of the order of 0.1-0.5 per formula unit. This raises the interesting question of how ferromagnetism develops in the pyrochlores, and whether the double-exchange interaction is the only mechanism operative for stabilizing the ferromagnetic and metallic states [38].

#### CMR in thin films

In 1993, Von Helmolt et al. reported a large, room-temperature magnetoresistance effect in La $_{0.7}$ Ba $_{0.3}$ MnO $_3$  epitaxial thin films made using pulsed laser deposition (PLD) in an off-axis geometry. This geometry reduces the number of particles formed on the film surface—deposition of particles a few thousand angstroms to a micron in size is a problem associated with laser deposition. On-axis deposition with a sintered-powder ceramic target typically results in a particle density of the order of  $\sim 10^5$ – $10^6$  cm $^{-2}$ . Off-axis deposition is known to reduce the powder density by at least an order of magnitude [40]. Ceramic targets with stoichiometric

<sup>&</sup>lt;sup>h</sup>Polycrystalline ceramic.

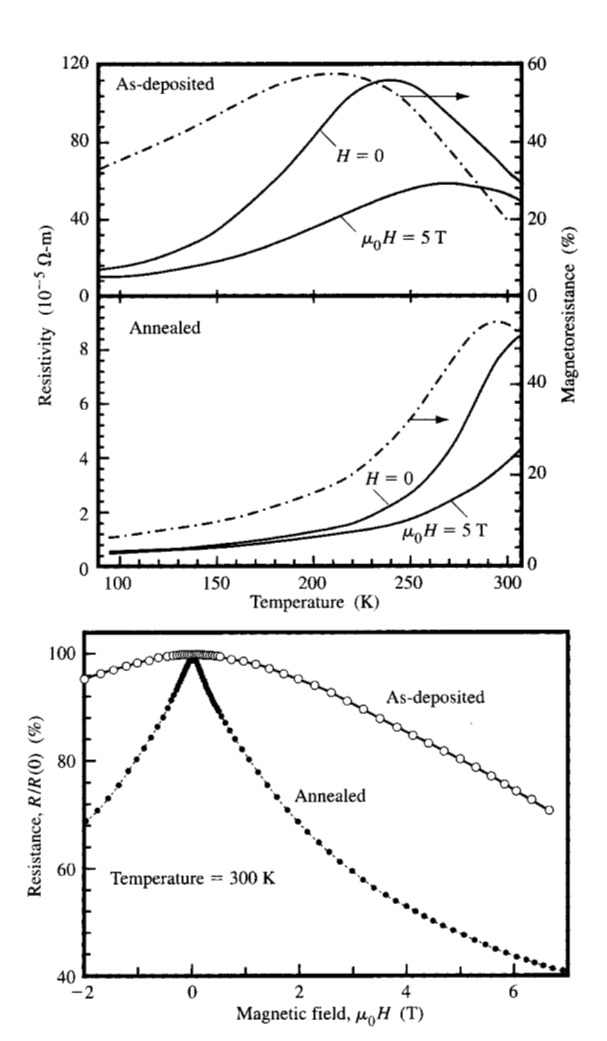
composition were used. The substrates were SrTiO<sub>3</sub> single crystal, (100) or (110) cut. Optimal deposition was obtained at a substrate temperature of 600°C, in an oxygen background pressure of 300 mTorr. Curiously, they reported that higher substrate temperature resulted in polycrystalline films, which was not a commonly seen phenomenon. As-deposited films show paramagnetic response at room temperature. A subsequent anneal at 900°C in air for 12 hours resulted in a marked increase in Curie temperature. The sample becomes ferromagnetic at room temperature, although its magnetic moment at 2 tesla is still only 89% of that observed in bulk material. A magnetoresistance of  $\Delta R/R(H=7\text{ T}) \sim 150\%$  was seen, as summarized in Figure 4.

Jin et al. [7] and McCormack et al. [6] reported the synthesis of epitaxial La<sub>0.67</sub>Ca<sub>0.33</sub>MnO<sub>3</sub> films that exhibited a field-driven change of resistivity of three orders of magnitude in a field of 6 tesla. Their films were about 1000 Å thick, deposited using pulsed laser ablation on (100) LaAlO<sub>3</sub> substrates. Their optimal deposition temperature was 650-700°C in an oxygen atmosphere of 100-300 mTorr. The highest magnetoresistance, shown in Figure 1, was obtained by heat-treating the films after deposition at 900°C for 30 min in 3 atm. of oxygen [6]. A large CMR effect in Nd<sub>0.7</sub>Sr<sub>0.3</sub>MnO<sub>3-δ</sub> thin films was reported by Xiong et al. [41]. Their films were prepared using laser ablation in 300 mTorr of N<sub>2</sub>O. The substrate temperature was in the range of 600-800°C during deposition. Trajanovic et al. reported successful growth of La<sub>0.67</sub>Sr<sub>0.33</sub>MnO<sub>3</sub> thin films on buffered silicon substrates using laser ablation [42]. Many more thin-film materials systems have since been investigated.

Commonly used deposition techniques for perovskite oxide deposition include laser ablation, reactive sputtering, reactive ion beam sputtering, co-evaporation, and CVD.

Table 2 gives a summary of some recent publications on efforts of synthesizing the doped manganate perovskites using these techniques and the basic properties of the resulting films.

Laser ablation is most widely used in a laboratory environment for the deposition of oxides. It is by far the most straightforward deposition method for complex oxides because of the ease of obtaining stoichiometric transfer of materials from target to substrate. Deposition can be made in various gas atmospheres within a wide pressure range, typically from 0 to 1 Torr. The major drawback for laser ablation is its scalability. Deposition of films over a 2-in. diameter would require major engineering effort. Because of the short target-to-substrate distance (typically around 2 in.), it is currently very difficult to imagine laser ablation being scaled up for deposition of wafers of a size much larger than 4 in. in diameter. Another problem associated with laser ablation is the generation of particulates. These particles, typically



## First report of large negative magnetoresistance in La<sub>0.7</sub>Ba<sub>0.3</sub>MnO<sub>3</sub> thin films. Annealing of a thin-film La<sub>0.7</sub>Ba<sub>0.3</sub>MnO<sub>3</sub> at 900°C was shown to increase its Curie temperature and enhance its magnetoresistance. Redrawn from [3], with permission.

 $0.1-1~\mu m$  in size, could seriously affect the yield of devices at a high device density.

Reactive sputtering excels in the deposition of largearea films. Deposition of oxide films, especially complex oxides involving more than one cation element, could become challenging because of the problem of nonstoichiometric transfer. Both the sputtering process at the target and the resputtering process at the substrate can affect the stoichiometry of resulting films. For oxides containing alkaline metal cations, large amounts of oxygen negative ions can be generated at the target. The resputtering effect of these negative ions at the substrate is to alter the resulting film composition from that of the

**Table 2** Some recent results on thin-film CMR materials. In the *Material* column, only cation ratios are listed. T denotes target composition, F denotes film composition, and  $T_s$  denotes deposition temperature. Results from as-grown films are denoted with a superscript a when necessary. Superscripts b and c correspond to different annealing conditions.  $T_p$  denotes the resistance-peak temperature. Room-temperature resistivity is denoted as  $\rho_0$ .

Material	Deposition	Substrate	$T_{ m s}$	Pressure	Annealing	$a_0$	$T_{p}$	$ ho_0$	Maximum
	method		(°C)	(mTorr)	conditions	(Å)	(K)	(Ω-cm)	$\Delta R/R(H)$
T: La <sub>0.7</sub> Ba <sub>0.3</sub>	Off-axis PLD [3]	SrTiO <sub>3</sub> (100) (110)	600	300	900°C 12 hr air	N/A	~300	$3 \times 10^{-4}$	150% at 7 T
T: La <sub>0.67</sub> Ca <sub>0.33</sub>	PLD [7]	LaAlO <sub>3</sub> (100)	~600-700	100 (O <sub>2</sub> )	$700^{\circ}$ C/30 min <sup>b</sup> $900^{\circ}$ C/3 hr <sup>c</sup> 1 atm O <sub>2</sub>		$\sim 100^{a}  \sim 200^{b}  \sim 280^{c}$	N/A	$\begin{array}{cccc} 460\%^a & 1400\%^b \\ 400\%^c & 10^5\%^{\text{best}} \\ & \text{at 6 T} \end{array}$
T: La <sub>0.67</sub> Ca <sub>0.33</sub>	PLD [6]	LaAlO <sub>3</sub> (100)	~650-700	~100- 300 (O <sub>2</sub> )	900°C 30 min 3 atm O <sub>2</sub>	3.89 <sup>a</sup>	~100	N/A	1.25 × 10 <sup>5</sup> % at 6 T
T: La <sub>0.7</sub> Ca <sub>0.3</sub>	PLD [24, 43]		720	150 (O <sub>2</sub> )	none	3.855	220	$1 \times 10^{-2}$	
T: La <sub>0.7</sub> Ba <sub>0.3</sub>	PLD [24, 43]		720	$150 (O_2)$	none	3.885	330	$1 \times 10^{-4}$	
T: Y <sub>0.7</sub> Sr <sub>0.3</sub>	PLD [24, 43]	MgO	720	$150 (O_2)$	none	3.858	360	$5 \times 10^{-6}$	
T: La <sub>0.7</sub> Sr <sub>0.3</sub>	PLD [24, 43]	(100)	720	$150 (O_2)$	none	3.875	370	$6 \times 10^{-5}$	
T: Nd <sub>0.7</sub> Sr <sub>0.3</sub>	PLD [24, 43]		720	150 (O <sub>2</sub> )	none	3.872	115	$8 \times 10^3$	
$T: Nd_{0.7}Ba_{0.3}$	PLD [24, 43]		720	150 (O <sub>2</sub> )	none	3.885	110	$8 \times 10^5$	
T: Nd <sub>0.7</sub> Sr <sub>0.3</sub>	PLD [41]	LaAlO <sub>3</sub> (100)	~600-800	300 (N <sub>2</sub> O)	$900^{\circ}$ C 30 min 1 atm O <sub>2</sub>	3.93 <sup>a</sup>	(95°) 50	$2 \times 10^{-2}$	3340% <sup>a</sup> at 5 T $\ge 10^6$ % at 8 T
T: La <sub>0.67</sub> Ca <sub>0.33</sub>	PLD [44]	LaAlO <sub>3</sub> (100)	700	100 (O <sub>2</sub> )	$850^{\circ}\text{C}$ 1 hr, 3 atm $\text{O}_2$	N/A	110	N/A	$1.1 \times 10^6\%$ at 6 T
T: $La_{0.68}Ca_{0.11}$ F: $La_{0.72}Ca_{0.25}$	Ion beam sputter [17], 1 kV/80 mA	MgO (100)	N/A	$0.25$ $Xe:O_2 = 1:1.5$	N/A	3.90	220	$<1 \times 10^{-2}$	120% at 1 T
F: La <sub>0.74</sub> Pb <sub>0.26</sub>	rf sputter [45], 2 in., 50 W	Si (100)	500	$40$ Ar: $O_2 = 4:1$	800°C 2 hr, O <sub>2</sub>	3.86	325	$3 \times 10^2$	30% at 2 T
T: La <sub>0.67</sub> Ca <sub>0.33</sub>	dc sputter [46], 380 V/100 mA	MgO (100)	700	$Ar:O_2 = 1:1$		a = b = 7.76 $c = 7.74$		12	460% at 0.82 T
T: La <sub>0.67</sub> Ca <sub>0.33</sub>	dc sputter [46], 380 V/100 mA	MgO (100)	700	60 Ar:O <sub>2</sub> = 1:1	950°/C 6 hr, air		226	$< 10^{-3}$	130% at 0.82 T
F: La <sub>0.67</sub> Ca <sub>0.33</sub>	MOCVD [23]	LaAlO <sub>3</sub> (100)	~500-700	3–4 Torr (O <sub>2</sub> )	$950^{\circ}$ C $\sim$ 1 hr (1 atm O <sub>2</sub> )	N/A	~260	$2 \times 10^{-4}$	42% at 7 T
F: La <sub>0.67</sub> Sr <sub>0.33</sub>	MOCVD [23]	$\begin{array}{c} \text{LaAlO}_3 \\ (100) \end{array}$	~500-700	3–4 Torr (O <sub>2</sub> )	$$950^{\circ}C$$ $\sim$ 1 hr (1 atm $O_{2})$	N/A	380	$1.5 \times 10^{-4}$	27% at 7 T
F: La <sub>0.58</sub> Ca <sub>0.33</sub>	MBE [47]	SrTiO <sub>3</sub> (100)	680	0.01 O-zone	as grown	3.815	234	N/A	900% at 5.5 T
T: La <sub>0.75</sub> self-doped	PLD [31]	SrTiO <sub>3</sub> (100)	~600-700	250 (O <sub>2</sub> )	as grown <sup>a</sup> and 850°C	N/A		$2 \times 10^{-4}$ a	425%" at 4 T
					30 min (O <sub>2</sub> )		315	N/A	130% at 4 T
T: La <sub>0.67</sub> Sr <sub>0.33</sub>	PLD [42]	Si (100) Bi <sub>4</sub> Ti <sub>3</sub> O <sub>12</sub> buffered	670	400	as grown	3.88	380	$1 \times 10^{-4}$	N/A
T: La <sub>0.67</sub> Ca <sub>0.33</sub>	PLD [48]	Si (100) (111) YSZ	~600-750	200 (O <sub>2</sub> )	as grown	3.83	~120- 210	$\sim 2-4 \times 10^{-2}$	250% at 5 T
		buffered							

target. There is evidence, however, that this problem may not be as serious for manganates as it is in the case of high-temperature superconducting cuprates—to the extent that one may not have to use off-axis sputtering to get good enough stoichiometric transfer [5, 45, 46].

For large-area deposition, reactive molecular beam epitaxy using thermal evaporation has been gaining momentum in recent years [47, 49–54]. MOCVD has also been successfully applied to the growth of manganates [23]. Bae and Wang have reported successful synthesis of La<sub>0.67</sub>Ca<sub>0.33</sub>MnO<sub>3</sub> epitaxial thin films using a sol-gel approach [55].

Most commonly used substrates are perovskite single crystals of SrTiO<sub>3</sub> and LaAlO<sub>3</sub>. This is because a good lattice match to the manganates is required. There is, however, some recent progress in the successful growth of high-quality epitaxial thin films on buffered silicon substrates [42, 45, 48], which might be more interesting for technological reasons.

One striking feature of the manganate thin films is the sensitivity of their properties to postdeposition heat treatment, as can be seen clearly from the data presented in Table 2. This is probably related to the strong mutual dependence of the magnetic state and the local lattice configuration, especially that of the Mn-O-Mn bond length and bond angle, as has previously been discussed. Direct comparison of data is difficult between thin-film and bulk samples, either single-crystal or polycrystalline, because of the possible existence of a large amount of residual uniaxial stress in thin films. For manganate films that are epitaxial, their precise cell dimensions and structures cannot be determined completely from simple  $\theta$ –2 $\theta$  X-ray diffraction. This may contribute partially to the lack of direct correlation between their  $T_n$  and lattice parameters, as shown in Table 2.

There might be some interaction between the grain boundaries and the magnetic domain boundaries that could lead to the pinning of magnetic domain boundaries at the grain boundary, resulting in increased spin-dependent scattering of carriers at the grain boundary [56]. On the whole, however, the role of the grain boundary is much less significant for the transport properties of manganate thin film than it is for high-temperature superconducting cuprates. This is also evident from the fact that similar magnetotransport properties can be obtained from epitaxial thin films and polycrystalline bulk samples with only minor tuning of the processing conditions.

#### **Magnetic properties**

The saturation magnetic moment of  $\text{La}_{1-x}\text{Ca}_x\text{MnO}_3$  peaks around x=0.3 [18]. This moment corresponds to about 3.6 Bohr magnetons ( $\mu_B$ ) per Mn site, or a low-temperature saturation magnetization of  $4\pi M \approx 7400$  Oe.

As-grown films appear to be fairly soft magnetically, with a coercivity of the order of 10-500 Oe, depending on the type of material, its growth condition, and the operating temperature.

The magnetization of most laser-deposited films appears to lie in the film plane, as one would expect from the large shape anisotropy. It is not yet clear whether there are preferential directions for the magnetic moment to align in-plane. Optical Kerr contrast microscopy [19] on as-grown La<sub>0.67</sub>Sr<sub>0.33</sub>MnO<sub>3</sub> thin films shows a possible inplane easy axis along the pseudocubic cell axis of the manganates, at least over an area tens of microns in size. No significant difference is seen, however, in magnetic hysteresis loops of samples several millimeters in size when the field is aligned in the (100) or (110) direction of the pseudocubic axis. Uniaxial strain or stress in films can also complicate matters to some degree. Observation of perpendicular magnetic anisotropy in sputter-deposited  $La_{1-x}Sr_xMnO_3$  polycrystalline films with x = 0.21 has been reported by Cho et al. [5].

A significant amount of linewidth broadening in the ferromagnetic resonance spectrum was observed [57] for as-grown thin films of  $\text{La}_{0.67}\text{Ba}_{0.33}\text{MnO}_3$ , suggesting the presence of magnetic inhomogeneity. High-temperature annealing of the films reduces their FMR linewidth and the dc resistivity. An extrapolated zero-temperature spinwave stiffness constant of  $D(0) \approx 115 \text{ meV-Å}^2$  was obtained for  $\text{La}_{0.67}\text{Ca}_{0.33}\text{MnO}_3$  thin films at 10 GHz. This agrees with the estimate obtained from recent neutron diffraction studies [58].

#### Possible origins of CMR

Goodenough et al. [59, 60] proposed a qualitative theory for the magnetic interaction in the manganates based on a special type of covalent Mn-O-Mn bond, which he denotes as the semicovalent bond. For this type of bond, the distance between the ions is very important. For magnetic moments of ions sharing the oxygen ion, a small lattice constant would lead to antiparallel or negative exchange coupling, while a longer bond length would lead to parallel or positive exchange coupling. For the doped manganate perovskite family of compounds, there is a weak magnetic exchange coupling between the Mn<sup>3+</sup> ions, a negative interaction between the Mn<sup>4+</sup> ions, and a strong positive interaction between the Mn3+ and Mn4+ ions [14]. The type and strength of magnetic exchange coupling between adjacent manganese ions in the Mn-O-Mn bond depends sensitively on the valency of the Mn, or the doping level x of the compound.

One peculiar feature of the doped manganate perovskites is the close association of ferromagnetism with metallic conduction. Zener [61] proposed the mechanism of double exchange that could explain this correlation. Doping of the trivalent rare-earth site by divalent ions

causes a corresponding number of Mn<sup>3+</sup> ions to become Mn<sup>4+</sup>. The displacement of these holes (sometimes referred to as Zener carriers [62]) increases the conductivity. The strong positive exchange coupling between the Mn<sup>3+</sup> and Mn<sup>4+</sup> ions in Mn<sup>3+</sup>-O-Mn<sup>4+</sup> provides a mechanism for ferromagnetic ordering. A resonance hybrid between the two states  $\Psi_1$ :  $Mn^{3+}-O^{2-}-Mn^{4+}$  and  $\Psi_2$ :  $Mn^{4+}-O^{2-}-Mn^{3+}$  is energetically favored. For such a simplified model, the transfer integral for one electron becomes [63, 64]  $t_{ij} = b_{ij} \cos(\theta_{ij}/2)$ , where  $\theta_{ii}$  is the angle between the two ionic spins and  $b_{ii}$  is the coupling constant. When considered in the environment of an extended lattice, this interplay between dopant level and the magnetic ground state leads to the theoretical proposal of either a canted or a spiral ground state for the Mn spin, with  $\theta_{ii}$  determined by dopant concentration x [65].

Double exchange provides a mechanism for the explanation of the simultaneous onset of metallicity and ferromagnetism. On the other hand, Millis et al. [66] showed that a Hamiltonian containing only double exchange is insufficient to account for the large magnetoresistance observed in these CMR compounds. The calculated resistance is too small. It has an incorrect temperature and field dependence when compared with experiment. They concluded that a strong electron-phonon interaction, in this case mediated by the Jahn-Teller coupling of the Mn<sup>3+</sup> ions, must be included. The 3d4 Jahn-Teller distortion of Mn<sup>3+</sup> is known to be strong. With a Jahn-Teller energy of the order of [66] 1 eV, it is the underlying driving force for the tetragonalto-orthorhombic phase transition observed for  $x \le 0.2$ , as was shown in Figure 3(a). It is also responsible for the cubic-tetragonal transition observed at  $T^* \approx 800 \text{ K}$  in LaMnO<sub>3</sub> [59]. Roder et al. [67] presented a calculation that incorporated the coupling to longitudinal optical phonons in the double exchange model, and showed that such coupling causes a suppression of the mean-field magnetic transition temperature, with the amount of suppression dependent on the Jahn-Teller coupling strength. Millis et al. [68] suggested that for x > 0.2and above Curie temperature, slowly fluctuating local Jahn-Teller distortions localize the conduction-band electrons into polarons. The polaron effect is turned off as temperature is decreased through  $T_a$ , permitting the formation of a metallic state. The competition between electron itineracy and self-trapping is controlled by the ratio of the Jahn-Teller self-trapping energy  $E_{\rm LT}$  and an electron itineracy energy which is parameterized by an effective hopping matrix element  $t_{eff}$ . Double exchange causes  $t_{\text{eff}}$  to be affected by the degree of magnetic order, and spin disorder leads to its reduction. When  $E_{\rm LT}/t_{\rm eff}$ exceeds a certain critical value, the phonon effect dominates and polarons form, localizing the electrons.

This "dynamic Jahn–Teller" polaron model is gaining support from some recent structural [35] and neutron diffraction studies. A large oxygen isotope effect on the ferromagnetic transition temperature in  $La_{0.8}Ca_{0.2}MnO_3$  was reported by Zhao et al. [69]. Evidence for polaron-dominated conduction was reported by Jaime et al. [70, 71]. Their recent transport measurements on  $La_{2/3}Ca_{1/3}MnO_3$  at temperatures above  $T_c$  revealed a large and field-independent difference between the activation energies for resistivity and for thermopower, which is a characteristic of Holstein polarons.

An explicit band calculation of the magnitude of Mn d-O p hybridization using local spin density approximation was recently reported by Pickett and Singh [16]. Their conclusions are as follows:

- 1. The electronic structure near the Fermi surface is found to be very nearly half metallic for  $La_{1-x}Ca_xMnO_3$  with x = 1/3.
- 2. A spin-dependent hybridization is found. For the minority channel, the O p bands and Mn d bands are nonoverlapping and hybridize much more weakly than is the case for the majority O p and Mn d bands that do overlap and mix very strongly at the Fermi level.
- 3. The Ca/La local environment disorder leads to variations in the Mn d site energy that create a tendency toward incoherence (i.e., localization) in the minority states near  $E_{\rm F}$ . These effects for the relatively broad majority bands should be minor. The likely result is that  $E_{\rm F}$  lies below a mobility edge, giving nonconducting minority states.
- 4. The half metallicity is a local effect that persists near flipped Mn spins (e.g., abrupt "domain walls"). The lack of a Stoner continuum and the possibility of minority spin polarons in a half-metallic ferromagnet provide possibilities for transport anomalies and for a large negative magnetoresistance.

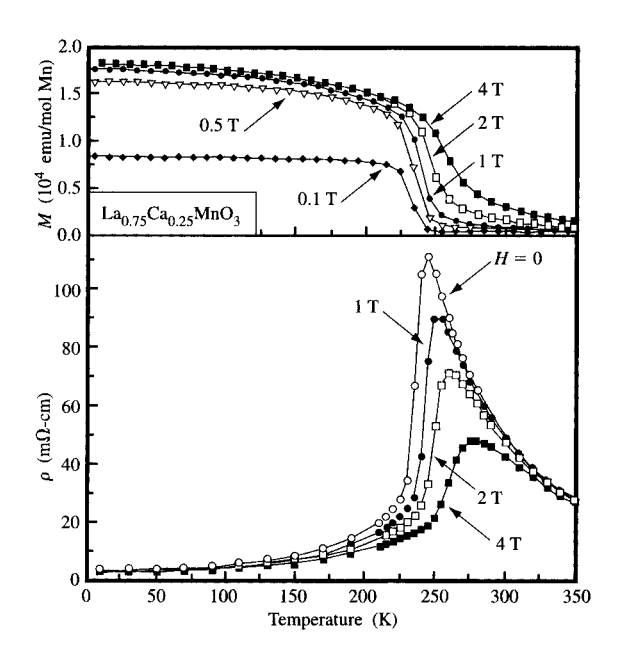
The strong field dependence of the magnetic properties suggests the presence of magnetic inhomogeneity. Experimentally, one finds that in an applied field of several tesla, the ferromagnetic transition broadens significantly, the low-temperature saturation magnetic moment increases, and a large reduction of resistance appears. An example is shown in Figure 5 for a set of data taken on a La<sub>0.75</sub>Ca<sub>0.25</sub>MnO<sub>3</sub> polycrystalline sample [20]. Zhang and Yang [72, 73] offered a theoretical model for the description of fluctuating magnetic clusters and their possible relation to magnetic excitations in the system. Sun et al. [74] analyzed this situation within a classical mean-field approximation [75]. The effective magnetic moment  $\mu$  at high field saturates at a value of around  $20~\mu_{\rm B}$ , suggesting a rather small ferromagnetic cluster containing only four or five Mn ions. There is also

evidence showing a possible correlation between the density of such magnetic clusters and the dopant concentration on the La site [74]. These magnetic clusters may be related to the Jahn-Teller distortion-based magnetic polaron described by Millis et al. [68]. In light of such a magnetically inhomogeneous system, the CMR effect may be related to the spin-dependent transport between these ferromagnetic (and thus metallic) clusters, with the amount of intercluster conductivity determined by the relative alignment of the magnetic moment of the clusters. As first pointed out by Byers and Rubinstein [76], this is similar to granular ferromagnetic tunneling systems such as Ni-SiO, [75], although here the mechanism for spin-dependent conductivity between clusters is still under investigation. Here, the large saturation field for CMR effect is simply a reflection of the small size of such magnetic clusters. If one could create a macroscopic interface for the relative rotation of magnetic moments from one side to another, one might expect large magnetoresistive effects for transport across such an interface. The field necessary to cause relative rotation of the macroscopic magnetic moment should be close to that of the coercivity of the manganate material, which is of the order of  $10^1$ – $10^2$  Oe. Thus, low-field CMR may be achievable.

The role of magnetic inhomogeneities has been fairly widely discussed in the literature (from different perspectives). For example, Ju et al. [77] investigated the correlation between magnetoresistance and magnetization in polycrystalline La<sub>0.67</sub>Ba<sub>0.33</sub>MnO<sub>3</sub> samples, and pointed out the possible importance of magnetic domain walls in determining the magnetoresistance. Hwang et al. [78] compared magnetoresistance of bulk single-crystal and polycrystalline La<sub>2/3</sub>Sr<sub>1/3</sub>MnO<sub>3</sub> samples, and suggested that spin-dependent tunneling might be responsible for intergranular transport in the polycrystalline samples; such a tunneling mechanism could be responsible for the additional low-field cusp in the magnetoresistance observed in the polycrystalline samples.

#### Low-field magnetoresistance

For the manganates to be useful in magnetic field sensing and memory applications, the saturation field of their CMR effect must be significantly reduced from its bulk value of several tesla. Cheong et al. [79], using a pair of ferromagnetic flux focusers attached to a ceramic piece of La<sub>0.67</sub>Ca<sub>0.33</sub>MnO<sub>3</sub> to locally concentrate magnetic field seen by the manganates, obtained a factor of 5900 enhancement of magnetoresistance response in fields below 10 Oe. An attempt at using a superconducting YBaCuO thin film to focus flux was made by Dong et al. [80]. Alternatively, Bozovic et al. [51, 81] used 2D MBE growth to fabricate lateral superlattices of manganates with different composition, so as to emphasize interface-

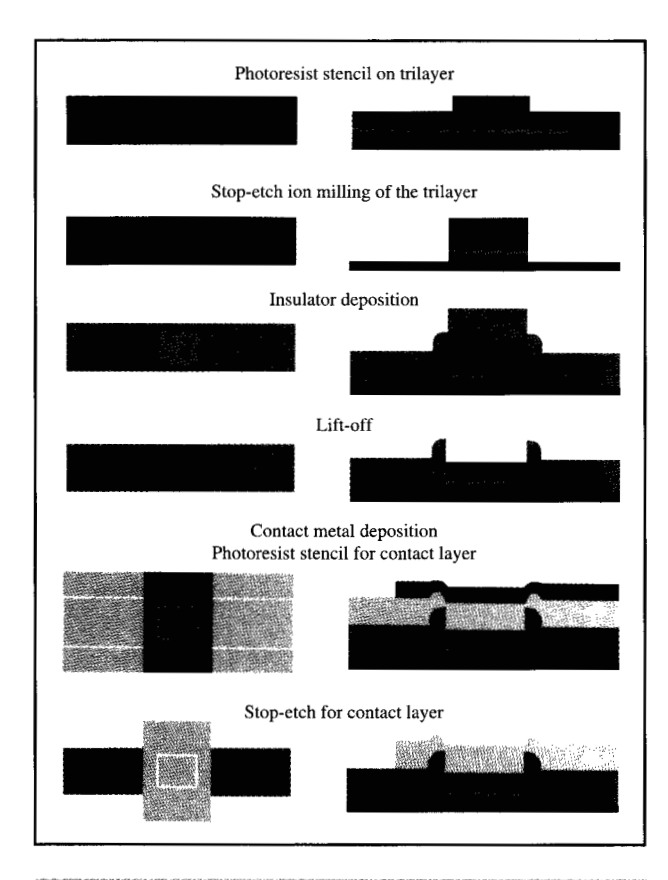


### Magnetic-field-dependent magnetization and resistivity as a function of temperature for a La<sub>0.75</sub>Ca<sub>0.25</sub>MnO<sub>3</sub> ceramic sample. Reproduced from [20], with permission.

related magnetic scattering of carriers. They observed an in-plane anisotropic resistance and reported a low-field magnetoresistance slope of (1/R)(dR/dH) = 36 per tesla [51].

The likelihood of strongly spin-dependent transport at an interface with misaligned magnetic moment prompts the search for isolation of a single interface by experimental means. Magnetic domain boundaries are considered natural candidates, and the observation of pinning of magnetic domain walls at grain boundaries has led to the investigation of magnetotransport studies in polycrystalline materials, as well as in thin films grown on polycrystalline substrates. Gupta et al. [56] investigated the possible consequences of magnetic domain boundary pinning by polycrystalline grain boundaries and observed an enhanced magnetoresistance in the low-temperature region compared to that observed for epitaxial thin films grown on single-crystal substrates.

Another approach is to fabricate a perpendicular transport structure with a trilayer thin film composed of underlying and overlying manganate layers, separated by a thin layer of foreign material so as to disrupt the magnetic exchange coupling but maintain some sort of electrical contact; and study the spin-dependent electrical transport across this structure using a current-perpendicular geometry. Sun et al. have successfully fabricated such a



Schematic of lithography process used to fabricate currentperpendicular magnetic trilayer structure.

structure to demonstrate a large low-field CMR effect [13]. A resistance change of a factor of 2 was obtained with a switching field of less than 200 Oe at 4.2 K. The structure was lithographically fabricated with  $La_{0.67}X_{0.33}MnO_3/SrTiO_3/La_{0.67}X_{0.33}MnO_3$  trilayers (with X = Ca, Sr). Figure 6 shows a schematic of the fabrication process. An example of the change in magnetoresistance as a function of sweeping field is shown in Figure 7. The mechanism of the spin-dependent transport process across  $SrTiO_3$  is yet to be fully understood. Nevertheless, the successful demonstration of such a device structure serves as an existence proof that a large magnetoresistive response can be achieved in low fields using the manganates.

Large low-field magnetoresistance has also been observed recently in layered manganite single-crystal La<sub>1.4</sub>Sr<sub>1.6</sub>Mn<sub>2</sub>O<sub>7</sub> by Kimura et al. [82]. Their transport measurement with current perpendicular to the Mn–O planes revealed a magnetoresistance as high as 240% in fields below 1 kOe and at temperatures below 100 K. They

suggested interplane spin-dependent tunneling as a possible mechanism for such low-field magnetoresistance.

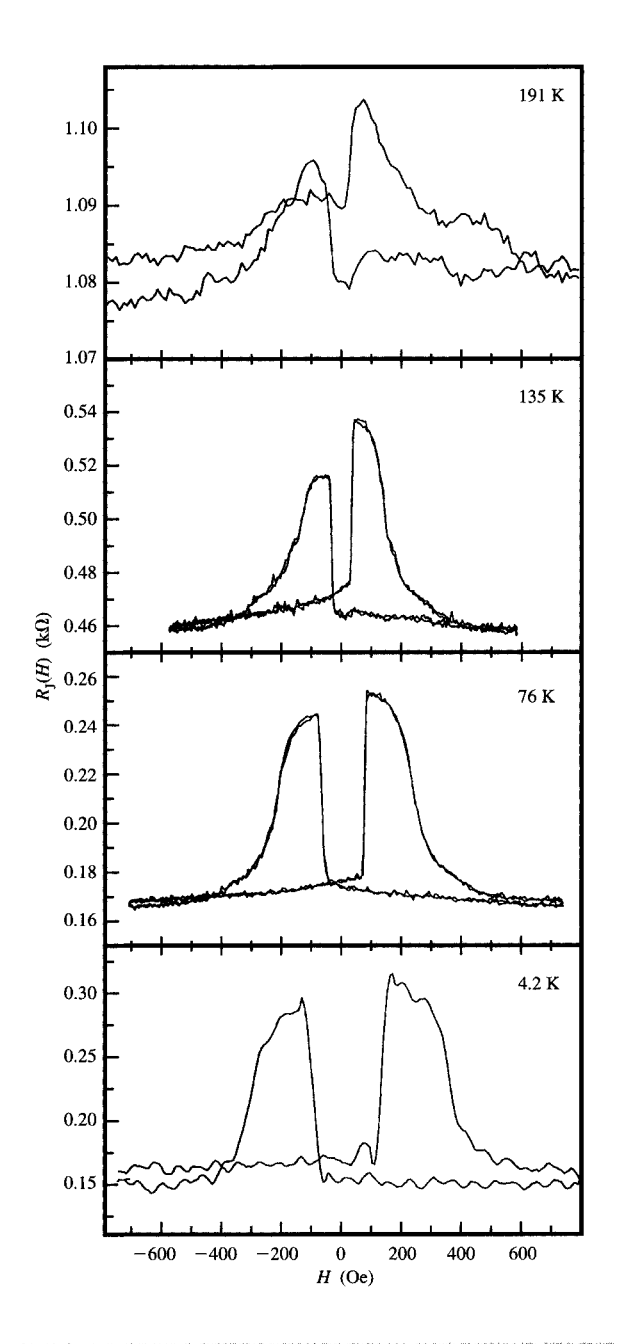
Thus far, large low-field magnetoresistance in the manganates has been observed only at reduced temperatures, usually below 100 K. One possibility is that at high temperatures, a large leakage current across a defect-populated barrier layer acts as a shunt to the magnetoresistance [83].

#### Summary

Interest in the doped perovskite manganates has been reactivated in the recent past. This followed from the observation of a large negative magnetoresistance in this class of materials, in thin-film form and at room temperature, which has made this class of materials potentially useful for magnetic-field-sensing applications such as hard-disk read heads. The magnitude of the magnetoresistance of the doped manganates can be orders of magnitude larger than that of metal alloy superlattices such as Cu/Co multilayers. The only other class of materials exhibiting such a large magnetoresistive effect is the class of magnetic semiconductors [84, 85] such as Eu, Gd Se. However, so far the effect there is limited to temperatures below 50 K. The large magnetoresistance of the doped manganates, however, persists to temperatures above ambient. For the generic doped manganate material to reach its full magnetoresistance, a saturation field of the order of a few tesla is usually needed. However, for certain device structures such as those involving use of a current-perpendicular trilayer transport junction, large magnetoresistances can be obtained at a low field.

The mechanism that governs the large spin-dependent transport in the doped manganates is not yet fully understood. It is likely that double exchange plays a central role in determining the local magnetic and electronic structure. However, there is ample evidence for the presence of magnetic inhomogeneities, perhaps coupled to local structural distortions in forms of magnetic polarons mediated through a Jahn-Teller distortion-based electron-phonon coupling. The magnetic interaction of these local magnetic clusters resembles that of a granular magnetic system, and the spin-dependent electronic transport across these local magnetic clusters is probably the origin of the large magnetoresistive effect.

Large low-field magnetoresistance has been demonstrated only at reduced temperature. The noise characteristic of the doped manganates is still under investigation; preliminary studies show the presence of large 1/f noise, perhaps due to magnetic domain wall motions [86–88]. The high-frequency response of their magnetoresistance would have to be determined, and associated fabrication processes compatible with the microelectronics technology would have to be developed



Magnetoresistance across a La $_{0.67}$ Sr $_{0.33}$ MnO $_3$ /SrTiO $_3$ /La $_{0.67}$ Sr $_{0.33}$ MnO $_3$  trilayer structure. The SrTiO $_3$  is nominally 50 Å thick and interrupts the exchange coupling between the upper and lower La $_{0.67}$ Sr $_{0.33}$ MnO $_3$  layers, allowing the moment of one to rotate freely with respect to the other. Junction area: 3  $\mu$ m  $\times$  5.5  $\mu$ m. The substrate for this structure was a (100) cut single crystal of SrTiO $_3$ . Reproduced from [13], with permission.

before the applicability of this class of materials to magnetic sensing applications could be assessed.

#### **Acknowledgments**

We wish to thank J. C. Slonczewski, D. P. DiVincenzo, J. J. Connolly, S. L. Brown, R. A. Altman, L. S. Yu-Jahnes, C. Jahnes, Yu Lu, G. Q. Gong, R. B. Laibowitz, D. B. Mitzi, R. H. Koch, C. C. Tsuei, John Kirtley, and M. B. Ketchen of the IBM Thomas J. Watson Research Center; M. Rubinstein of the Naval Research Laboratories; and Dan Lathrop and Steve Haupt of Quantum Magnetics Inc. for helpful discussions and assistance during various stages of our work on this subject. One of us (G. X.) wishes to acknowledge support from the National Science Foundation under Grant No. DMR-9414160.

#### References

- R. M. Kusters, J. Singleton, D. A. Keen, R. McGreevy, and W. Hayes, *Phys. B* 155, 362 (1989).
- C. W. Searle and S. T. Wang, Can. J. Phys. 48, 2023 (1970).
- 3. R. von Helmolt, J. Wecker, B. Holzapfel, L. Schultz, and K. Samwer, *Phys. Rev. Lett.* 71, 2331 (1993).
- M. Kasai and T. Ohno, Jpn. J. Appl. Phys. 29, L2219 (1990).
- J. Cho, M. Gomi, and M. Abe, *Jpn. J. Appl. Phys.* 29, 1686 (1990).
- M. McCormack, S. Jin, T. H. Tiefel, R. M. Fleming, Julia M. Philips, and R. Ramesh, Appl. Phys. Lett. 64, 3045 (1994).
- S. Jin, T. H. Tiefel, M. McCormack, R. A. Fastnacht, R. Ramesh, and L. H. Chen, Science 264, 413 (1994).
- 8. S. Jin, M. O'Bryan, T. H. Tiefel, M. McCormack, and W. W. Rhodes, *Appl. Phys. Lett.* **66**, 382 (1995).
- J. Z. Sun, L. Krusin-Elbaum, S. S. P. Parkin, and G. Xiao, Appl. Phys. Lett. 67, 2726 (1995).
- G. C. Xiong, S. C. Wu, D. S. Dai, B. Zhang, Z. X. Lu,
   G. J. Lian, Z. Z. Gan, Q. Li, H. L. Ju, J. Wu, L. Senapati,
   R. L. Greene, and T. Venkatesan, *Phys. Rev. B* (preprint) (1997).
- 11. M. F. Hundley, M. Hawley, R. H. Heffner, Q. X. Jia, J. J. Neumeier, J. Tesmer, J. D. Thompson, and X. D. Wu, *Appl. Phys. Lett.* **67**, 860 (1995).
- M. F. Hundley, J. J. Neumeier, R. H. Heffner, Q. X. Jia,
   X. D. Wu, and J. D. Thompson, J. Appl. Phys. 79, 4535 (1996).
- J. Z. Sun, W. J. Gallagher, P. R. Duncombe,
   L. Krusin-Elbaum, R. A. Altman, A. Gupta, Y. Lu, G. Q. Gong, and G. Xiao, Appl. Phys. Lett. 69, 3266 (1996).
- 14. G. H. Jonker, Physica XXII, 707 (1956).
- 15. G. H. Jonker and J. H. V. Santen, Physica XVI, 337 (1950).
- W. E. Pickett and D. J. Singh, *Phys. Rev. B* 53, 1146 (1996).
- K.-I. Chahara, T. Ohno, M. Kasai, and Y. Kozono, *Appl. Phys. Lett.* 63, 1990 (1993).
- E. O. Wollan and W. C. Koehler, *Phys. Rev.* **100**, 545 (1955).
- P. Lecoeur, P. L. Trouilloud, G. Xiao, A. Gupta, G. Q. Gong, and X. W. Li, J. Appl. Phys. 82, 3934 (1997).
- P. Schiffer, A. P. Ramirez, W. Bao, and S.-W. Cheong, *Phys. Rev. Lett.* 75, 3336 (1995).
- R. von Helmolt, J. Wecker, K. Samwer, and K. Barner, J. Magn. Magn. Mater. 151, 411 (1995).
- H. L. Ju, C. Kwon, Q. Li, R. L. Greene, and T. Venkatesan, *Appl. Phys. Lett.* 65, 2108 (1994).
- G. J. Snyder, R. Hiskes, S. DiCarolis, M. R. Beasley, and T. H. Geballe, *Phys. Rev. B* 53, 14,434 (1996).
- J. M. D. Coey, M. Viret, L. Ranno, and K. Ounadjela, *Phys. Rev. Lett.* 75, 3910 (1995).

- H. Kuwahara, Y. Tomioka, Y. Moritomo, A. Asamitsu, M. Kasai, R. Kumai, and Y. Tokura, Science 272, 80 (1996).
- 26. Y. Tokura, H. Kuwahara, Y. Moritomo, Y. Tomioka, and A. Asamitsu, *Phys. Rev. Lett.* **76**, 3184 (1996).
- 27. Y. Tomioka, A. Asamitsu, Y. Moritomo, H. Kuwahara, and Y. Tokura, *Phys. Rev. Lett.* 74, 5108 (1995).
- 28. J. Barratt, M. R. Lees, G. Balakrishnan, and D. M. Paul, *Appl. Phys. Lett.* **68**, 424 (1996).
- A. P. Ramirez, P. Schiffer, S.-W. Cheong, C. H. Chen, W. Bao, T. T. M. Palstra, B. Zegarski, P. L. Gammel, and D. J. Bishop, *Phys. Rev. Lett.* 76, 3188 (1996).
- J. A. M. van Roosmalen, P. van Vlaanderen, E. H. P. Cordfunke, W. L. IJdo, and D. J. W. IJdo, J. Solid State Chem. 114, 516 (1995).
- A. Gupta, T. R. McGuire, P. R. Duncombe, M. Rupp,
   J. Z. Sun, W. J. Gallagher, and G. Xiao, *Appl. Phys. Lett.* 67, 3494 (1995).
- 32. H. Y. Hwang, T. T. M. Palstra, S.-W. Cheong, and B. Batlogg, *Phys. Rev. B* **52**, 15,046 (1995).
- Z. Arnold, K. Kamenev, M. R. Ibarra, P. A. Algarabel, C. Marquina, J. Blasco, and J. Garcia, *Appl. Phys. Lett.* 67, 2875 (1995).
- K. Khazeni, Y. X. Jia, L. Lu, V. H. Crespi, M. L. Cohen, and A. Zettl, *Phys. Rev. Lett.* 76, 295 (1996).
- P. G. Radaelli, D. E. Cox, M. Marezio, S.-W. Cheong,
   P. E. Schiffer, and A. P. Ramirez, *Phys. Rev. Lett.* 75, 4488 (1995).
- A. Asamitsu, Y. Moritomo, Y. Tomioka, T. Arima, and Y. Tokura, *Nature* 373, 407 (1995).
- Y. Moritomo, A. Asamitsu, H. Kuwahara, and Y. Tokura, Nature 380, 141 (1996).
- 38. Y. Shimakawa, Y. Kubo, and T. Manako, *Nature* **379**, 53 (1996).
- M. A. Subramanian, B. H. Toby, A. P. Ramirez, W. J. Marshall, A. W. Sleight, and G. H. Kwei, *Science* 273, 81 (1996).
- B. Holzapfel, B. Roas, L. Schultz, P. Bauer, and G. Saemann-Ischenko, Appl. Phys. Lett. 61, 3178 (1992).
- G. C. Xiong, Q. Li, H. L. Ju, S. N. Mao, L. Senapati, X. X. Xi, R. L. Greene, and T. Venkatesan, *Appl. Phys. Lett.* 66, 1427 (1995).
- Z. Trajanovic, C. Kwon, M. C. Robson, K.-C. Kim, M. Rajeswari, R. Ramesh, T. Venkatesan, S. E. Lofland, S. M. Bhagat, and D. Fork, *Appl. Phys. Lett.* 69, 1005 (1996).
- J. F. Lawler, J. G. Lunney, and J. M. D. Coey, *Appl. Phys. Lett.* 65, 3017 (1994).
- L. H. Chen, S. Jin, T. H. Tiefel, R. Ramesh, and D. Schurig, *IEEE Trans. Magn.* 31, 3912 (1995).
- G. Srinivasan, V. S. Babu, and M. S. Seehra, Appl. Phys. Lett. 67, 2090 (1995).
- X. T. Zeng and H. K. Wong, *IEEE Trans. Magn.* 31, 3910 (1995).
- 47. V. S. Achutharaman, P. A. Kraus, V. A. Vas'ko, C. A. Nordman, and A. M. Goldman, *Appl. Phys. Lett.* 67, 1019 (1995).
- 48. P.-J. Kung, D. B. Fenner, D. M. Potrepka, and J. I. Budnick, *Appl. Phys. Lett.* **69**, 427 (1996).
- J. N. Eckstein, I. Bozovic, J. O'Donnell, M. Onellion, and M. S. Rzchowski, Appl. Phys. Lett. 69, 1312 (1996).
- J. N. Eckstein, I. Bozovic, M. Rzchowski, J. O'Donnell, B. Hinaus, and M. Onellion, Proceedings of the Materials Research Society Epitaxial Oxide Thin Films II Symposium, 1996, p. 467.
- I. Bozovic and J. N. Eckstein, Appl. Surf. Sci. 113-114, 189 (1997).
- 52. P. Berberich, B. Utz, W. Prusseit, and H. Kinder, *Phys. C* **219**, 497 (1994).
- 53. H. Kinder, P. Berberich, B. Utz, and W. Prusseit, *IEEE Trans. Appl. Supercond. (USA)* 5, 1575 (1995).
- 54. J. O'Donnell, M. Onellion, M. S. Rzchowski, J. N. Eckstein, and I. Bozovic, *Phys. Rev. B* **54**, R6841 (1996).

- 55. S.-Y. Bae and S. X. Wang, Appl. Phys. Lett. 69, 121 (1996).
- A. Gupta, G. Q. Gong, G. Xiao, P. R. Duncombe, P. Trouilloud, P. Lecoeur, Y. Y. Wang, V. P. Dravid, and J. Z. Sun, *Phys. Rev. B* 54, R15629 (1996).
- S. E. Lofland, S. M. Ghagat, H. L. Lu, G. C. Xiong, T. Venkatesan, and R. L. Greene, *Phys. Rev. B* 52, 15,058 (1995).
- J. W. Lynn, R. W. Erwin, J. A. Borchers, Q. Huang, A. Santoro, J. L. Peng, and Z. Y. Li, *Phys. Rev. Lett.* 76, 4046 (1996).
- 59. J. B. Goodenough, Phys. Rev. 100, 564 (1955).
- J. B. Goodenough, A. Wold, R. J. Arnott, and N. Menyuk, *Phys. Rev.* 124, 373 (1961).
- 61. C. Zener, Phys. Rev. 82, 403 (1951).
- 62. R. von Helmolt, J. Wecker, K. Samwer, L. Haupt, and K. Barner, J. Appl. Phys. 76, 6925 (1994).
- 63. P. W. Anderson and H. Hasegawa, Phys. Rev. 100, 675 (1955).
- 64. P.-G. D. Gennes, Phys. Rev. 118, 141 (1960)
- 65. J. Inoue and S. Maekawa, Phys. Rev. Lett. 74, 3407 (1995).
- 66. A. J. Millis, P. B. Littlewood, and B. I. Shraiman, *Phys. Rev. Lett.* **74**, 5144 (1995).
- H. Roder, J. Zang, and A. R. Bishop, *Phys. Rev. Lett.* 76, 1356 (1996).
- A. J. Millis, B. I. Shraiman, and R. Mueller, *Phys. Rev. Lett.* 77, 175 (1996).
- G.-M. Zhao, K. Conder, H. Keller, and K. A. Muller, Nature 381, 676 (1996).
- M. Jaime, M. B. Salamon, M. Rubinstein, R. E. Treece,
   J. S. Horwitz, and D. B. Chrisey, *Phys. Rev. B* 54, 11,914 (1996).
- 71. M. Jaime, M. B. Salamon, K. Pettit, M. Rubinstein, R. E. Treece, J. S. Horwitz, and D. B. Chrisey, *Appl. Phys. Lett.* **68**, 1576 (1996).
- 72. S. Zhang, J. Appl. Phys. 79, 4542 (1996).
- 73. S. Zhang and Z. Yang, J. Appl. Phys. 79, 7398 (1996).
- J. Z. Sun, L. Krusin-Elbaum, A. Gupta, G. Xiao, and S. S. P. Parkin, *Appl. Phys. Lett.* **69**, 1002 (1996).
- J. I. Gittleman, Y. Goldstein, and S. Bozowski, *Phys. Rev.* B 5, 3609 (1972).
- J. Byers and M. Rubinstein, Bull. Amer. Phys. Soc. 40, 39 (1995).
- H. L. Ju, J. Gopalakrishnan, J. L. Peng, Q. Li, G. C. Xiong, and T. V. R. L. Greene, *Phys. Rev. B* 51, 6143 (1995).
- 78. H. Y. Hwang, S.-W. Cheong, N. P. Ong, and B. Batlogg, *Phys. Rev. Lett.* 77, 2041 (1996).
- S.-W. Cheong, H. Y. Hwang, and B. Batlogg, *Bull. Amer. Phys. Soc.* 41, 634 (1996).
- Z. W. Dong, T. Boettcher, C. H. Chen, I. Takeuchi, M. Rajeswari, R. P. Sharma, and T. Venkatesan, *Appl. Phys. Lett.* 69, 3432 (1996).
- 81. I. Bozovic, J. N. Eckstein, M. M. Rzchowski, J. O'Donnell, and M. Onellion, *Bull. Amer. Phys. Soc.* 41, 793 (1996).
- 82. T. Kimura, Y. Tomioka, H. Kuwahara, A. Asamitsu, M. Tamura, and Y. Tokura, *Science* 274, 1698 (1996).
- 83. J. Z. Sun, L. Krusin-Elbaum, P. R. Duncombe, A. Gupta, and R. B. Laibowitz, *Appl. Phys. Lett.* 70, 1769 (1997).
- S. V. Molnar, I. Terry, and T. Penney, presented at the Conference on IRC Superconductivity, Cambridge University, U.K., April 6-9, 1994.
- 85. S. Washburn, R. A. Webb, S. V. Molnar, F. Holtzberg, J. Flouquet, and G. Remenyi, *Phys. Rev. B* 30, 6224 (1984).
- H. T. Hardner, M. B. Weissman, M. Jaime, P. C. Dorsey, J. S. Horwitz, and D. B. Chrisey, *J. Appl. Phys.* 81, 272 (1997).
- 87. M. Rajeswari, A. Goyal, A. K. Raychaudhuri, M. C. Robson, G. C. Xiong, C. Kwon, R. Ramesh, R. L. Greene, T. Venkatesan, and S. Lakeou, *Appl. Phys. Lett.* **69**, 851 (1996).
- 88. G. B. Alers, A. P. Ramirez, and S. Jin, *Appl. Phys. Lett.* **68**, 3644 (1996).

Received November 11, 1996; accepted for publication March 14, 1997

Jonathan Z. Sun IBM Research Division, Thomas J. Watson Research Center, P.O. Box 218, Yorktown Heights, New York 10598 (JONSUN at YKTVMV, jonsun@watson.ibm.com). Dr. Sun is a Research Staff Member in the Physical Sciences Department at the IBM Thomas J. Watson Research Center. He received a B.S. degree in physics from Fudan University, Shanghai, China, in 1984, and M.S. and Ph.D. degrees in applied physics from Stanford University in 1986 and 1989, respectively. For the following two years, he worked at Superconductor Technologies Inc. in Santa Barbara, California, as a member of their technical staff. He subsequently joined IBM at the Thomas J. Watson Research Center, where he has worked on superconducting and magnetic thin films and devices. Dr. Sun is a member of the American Physical Society and the Materials Research Society.

Lia Krusin-Elbaum IBM Research Division, Thomas J. Watson Research Center, P.O. Box 218, Yorktown Heights, New York 10598 (ELBAUM at YKTVMV, elbaum@watson.ibm.com). Dr. Krusin-Elbaum received a Ph.D. degree in solid state physics from New York University in 1979. She subsequently joined the IBM Thomas J. Watson Research Center, where she is currently a Research Staff Member in the Physical Sciences Department. She has pursued her interests in a variety of subjects, such as spin-glasses, electronic transport in thin metal films, and semiconductor and superconducting devices. Since 1988, her efforts have been focused primarily on the exploration of the macroscopic magnetic behavior of high- $T_c$  superconductors. She has contributed to establishing basic superconducting parameters and to the understanding of the pinning of magnetic vortices and vortex dynamics in high-T<sub>o</sub> cuprate single crystals, films, and wires/tapes—important for future applications. Dr. Krusin-Elbaum is associated with an orders-of-magnitude enhancement of the current-carrying capability of the cuprate superconductors via doping with extended columnar defects by irradiation with high-energy heavy ions and GeV protons. Her current interests include the magnetic and transport properties of manganates and of small magnetic structures. Dr. Krusin-Elbaum has received four IBM Invention Achievement Awards, and she holds seven U.S. patents. She is a Fellow of the American Physical Society.

Arunava Gupta IBM Research Division, Thomas J. Watson Research Center, P.O. Box 218, Yorktown Heights, New York 10598 (AGUPTA at YKTVMV, agupta@watson.ibm.com). Dr. Gupta is a Research Staff Member in the Physical Sciences Department at the IBM Thomas J. Watson Research Center. He received an M.S. degree in chemistry from the Indian Institute of Technology in 1976 and a Ph.D. degree in chemical physics from Stanford University in 1980. He subsequently joined the Allied Signal Corporation in Morristown, New Jersey, where he worked on catalysis and laser processing of materials. In 1985 Dr. Gupta joined the Thomas J. Watson Research Center, where he has worked on various photothermal and photochemical laser techniques for processing and patterning of materials. His present interests are in areas related to the growth and properties of oxide thin films. He has pioneered the development and use of the pulsed-laser deposition technique for epitaxial and layer-bylayer growth of oxide films, for which he received an IBM Outstanding Technical Achievement Award in 1992. Dr. Gupta is a member of the Materials Research Society and the American Physical Society.

Gang Xiao Physics Department, Brown University, Providence, Rhode Island 02912 (xiao@physics.brown.univ). Dr. Xiao is an Associate Professor of Physics at Brown University in the areas of magnetism and high-vacuum thin-film deposition and characterization. He received M.Sc. and Ph.D. degrees in physics from The Johns Hopkins University, serving as a Postdoctoral Fellow there. He was a Sloan Research Fellow and a recipient of an NSF Young Investigator Award. In 1995 he received the Outstanding Young Scientist Award from the Overseas Chinese Physicists Association. Professor Xiao has published 102 journal articles in the area of condensed-matter physics and materials science. He has presented 30 invited talks at institutions and at national and international conferences. He holds a patent on magnetic recording media. Professor Xiao is a member of the American Physical Society.

Peter R. Duncombe IBM Research Division, Thomas J. Watson Research Center, P.O. Box 218, Yorktown Heights, New York 10598 (PRD at YKTVMV, prd@watson.ibm.com). Mr. Duncombe is a Senior Associate Engineer in the Exploratory Silicon Science and Technology Department at the IBM Thomas J. Watson Research Center, working on thin-film materials and processes for DRAM, MRAM, NVFRAM, and other applications of ferroelectric and high-permittivity ceramics. Since joining IBM in 1985, he has worked on sintering, superconductivity, GMR, and ceramic packaging. Mr. Duncombe received a Research Division Award for his contributions to the glass ceramic composite via in 1992 and a First Plateau Invention Achievement Award in 1995. He received a B.A. in chemistry from SUNY New Paltz in 1980 and an M.S. in chemical engineering from SUNY Buffalo in 1983. He is a member of the American Chemical Society.

Stuart S. P. Parkin IBM Research Division. Almaden Research Center, 650 Harry Road, San Jose, California 95120 (parkin@almaden.ibm.com). Educated in Britain, Dr. Parkin received his B.A. degree (1977) from the University of Cambridge, was elected a Research Fellow (1979) at Trinity College, Cambridge, and was awarded his Ph.D. degree (1980) at The Cavendish Laboratory, Cambridge. He joined IBM Research in San Jose as a World Trade Postdoctoral Fellow in 1982, becoming a permanent member of the staff the following year. Prior to coming to San Jose, he was awarded a Royal Society European Exchange Fellowship, which he spent as a Postdoctoral Fellow at the University of Paris, Orsay, in 1980 and 1981. At IBM, his interests have ranged from organic superconductors to ceramic high-temperature superconductors, and, in recent years, the study of magnetic thin-film structures and nanostructures. In 1991 Dr. Parkin discovered oscillations in the magnitude of the interlayer exchange coupling in transition-metal magnetic multilayered systems. In 1997 Dr. Parkin was awarded the Hewlett-Packard EuroPhysics Prize for Outstanding Achievement in Solid-State Physics for his "discovery and contribution to the understanding of Giant Magnetoresistance" and its "potential for technological applications." He has received other awards, including the Materials Research Society Outstanding Young Investigator Award (1991) and the Charles Vernon Boys Prize from the Institute of Physics, London (1991), as well as several awards from IBM, including three Outstanding Technical Achievement Awards and several awards for patents. He was elected a Member of the IBM Academy of Technology in 1997 and named a Master Inventor by the IBM Corporation in 1997. D. Parkin is a Fellow of the American Physical Society and a Consulting Professor at Stanford University. His work on magnetic multilayered structures is widely referenced. Recently it was reported in Science magazine that Dr. Parkin is the sixth most highly cited author in the physical sciences for the period 1990-1996. He was recently named a Centennial Lecturer by the American Physical Society. Dr. Parkin's present work involves the study of magnetic tunnel junctions and the development of an advanced nonvolatile magnetic random access memory based on magnetic tunnel junction storage cells.